

SUPPORTING INFORMATION

Supporting Information Table of Contents

Supporting Information Methods	2
Supporting Information Figures	7
Figure S1. Reaction mechanism for TET-dependent oxidation of 5mC-containing DNA.....	7
Figure S2. Synthesis of F27-4m5mC and F27-4dm5mC substrates.	7
Figure S3. ARP derivatization of F27-5mZ reaction products.	8
Figure S4. ESI-MS analysis of F27-4m5mC and F27-4dm5mC reaction products.	9
Figure S5. LC-MS/MS analysis of nucleoside products generated from reaction of TET2-CS with F27-5mC, F27-4m5mC and F27-4dm5mC.	10
Figure S6. Synthesis and characterization of F27-4mC and F27-4dmC substrates.....	12
Figure S7. ESI-MS analysis of TET reaction with potential alternative substrate.....	13
Figure S8. Characterization of convertible 4-(1,2,4-triazolyl)-5-methyl-dU phosphoramidite.....	15
Supporting Information Tables	16
Table S1. ESI-MS characterization of the potential substrates and products.	16
Supporting Information References	17

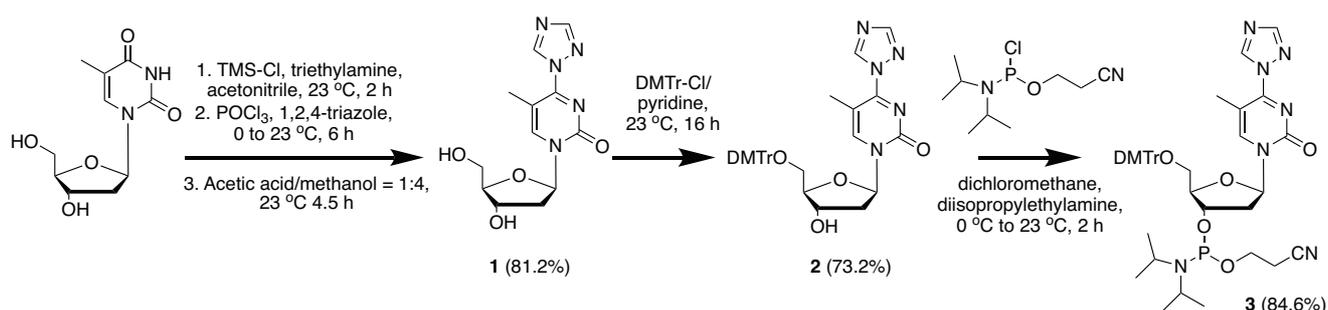
SUPPORTING INFORMATION

Supporting Information Methods

TET enzymes and expression plasmids. N-terminally FLAG-tagged TET2-CS, the crystal structure variant of the enzyme (1129-1936, Δ 1481-1843), was purified from insect cells as previously described.^[1] The constructs for full TET1 and TET3 catalytic domains (TET1-FCD and TET3-FCD) were cloned into pFastBac in a manner similar to TET2-CS, and baculovirus/insect cell purifications were also carried out in an identical manner as previously described.^[2]

General Synthetic Procedures. All reagents were purchased from Sigma Aldrich, Berry & Associates or Alfa Aesar. All anhydrous solvents were purchased in Sure/Seal bottles from Sigma Aldrich. High purity grade silica gel (230-400 mesh, 40-63 μ m particle size) from Sigma Aldrich was used for flash chromatography separation procedures. Merck 60 TLC (silica gel F₂₅₄) plates were used for reaction monitoring. All NMR experiments on the final phosphoramidite product were performed in deuterated acetonitrile (CD₃CN) solvent on a Bruker 400 MHz instrument. Chemical shift values are reported in parts per million (ppm) using the solvent peak (1.94 ppm for CD₃CN) as the reference. In interpreting the ¹H NMR peak multiplicities, s, d, t, q and m abbreviations were used for singlet, doublet, triplet, quartet, and multiplet, respectively. The ¹³C NMR spectra of the final compound is reported in ppm relative to the CD₃CN signal at 118.69 ppm. High resolution ESI-MS was performed in a Waters LCT Premier XE LC/MS system.

Synthesis of the convertible 4-(1,2,4-triazolyl)-5-methyl-dU CE phosphoramidite. 3'-O-(*N,N*-diisopropylamino-*O*- β -cyanoethoxyphosphino)-5'-O-(4,4'-dimethoxytrityl)-2'-deoxy-5-methyl-4-(1,2,4-triazolyl)-Uridine CE phosphoramidite (**3**) was synthesized via the following route:



The nucleoside (**1**) was synthesized following a previously reported procedure.^[3] Nucleoside **1** was then protected with a DMTr group on the 5'-OH. Briefly, in an oven dried round bottom flask (RBF) 295 mg (1 mmol, 1 eq) of 4-(1,2,4-triazolyl)-5-methyl-dU nucleoside was dissolved in 6 mL of anhydrous pyridine under argon atmosphere. Then, 350 mg (1 mmol, 1 eq) of 4,4'-dimethoxytrityl chloride (DMTr-Cl) was added and the reaction mixture was stirred for 8 h, after which an additional 175 mg (0.5 mmol, 0.5 eq) of DMTr-Cl was added and reaction was continued overnight (16 h) at room temperature (22 °C) under argon atmosphere. At completion, 5 mL of saturated sodium bicarbonate solution was added to the reaction mixture which was then extracted twice with 25 mL ethyl acetate. The organic layers were combined, washed with saturated sodium

SUPPORTING INFORMATION

chloride solution, and dried over anhydrous sodium sulfate. Solvent was removed in vacuo and crude product was purified by flash chromatography (hexane/ethyl acetate/triethylamine: 30/69/1 to 0/99/1; silica was suspended in hexane/ethyl acetate/triethylamine: 30/69/1 prior to use to prevent detritylation) to give 436 mg (73.2%) of **2** as a colorless foam. 240 mg of **2** (0.4 mmol, 1 eq) was then dissolved in 4 mL anhydrous methylene chloride and 420 μ L (6 eq, 2.4 mmol) *N,N*-diisopropylethylamine was added in an oven-dried RBF under argon atmosphere. Subsequently, 120 μ L (0.52 mmol, 1.3 eq) of 2-cyanoethyl *N,N*-diisopropylchlorophosphoramidite was added and reaction mixture stirred for 2 h at room temperature under argon atmosphere. Upon completion, solvent was removed in vacuo and crude product purified by flash chromatography (hexane/ethyl acetate/triethylamine: 30/69/1 to 0/99/1; silica was suspended in hexane/ethyl acetate/triethylamine: 30/69/1 prior to use to prevent detritylation) to give 269 mg (84.6%) of the final product **3** as a colorless foam. Final product was characterized by ^1H NMR (Figure S8A), ^{13}C NMR (Figure S8B), ^{31}P NMR and high resolution ESI-MS (HRMS). ^1H NMR (400 MHz, CD_3CN) δ (ppm): 9.30 (s, 1H, Ar), 8.44 (s, 1H, Ar), 8.13 (s, 1H, Ar), 7.48-7.41 (m, 2H, Ph), 7.37-7.27 (m, 6H, Ph), 7.20-7.26 (m, 1H, Ph), 6.91-6.82 (m, 4H, Ph), 6.22-6.16 (m, 1H, 1'-H), 4.65-4.55 (m, 1H, 4'-H), 4.17-4.0 (m, 2H, 5'-H), 3.85-3.69 (m, 7H, 3'-H, 2OCH₃), 3.62-3.25 (m, 4H, 2P-N-CH, P-O-CH₂), 2.79-2.63 (m, 3H, 2'-H, P-O-CH₂-CH₂), 2.47-2.35 (m, 1H, 2'-H), 2.0 (s, 3H, Ar-CH₃), 1.18-1.02 (m, 12H, 4CH₃). ^{13}C NMR (100 MHz, CD_3CN) δ (ppm): 160.2 (2C, PhC-OMe, DMTr), 154.6(2C, ArC, Ar), 148.4 (2C, ArC, Ar), 146.3-146.0 (3C, PhC, DMTr), 137 (1C, ArC, Ar), 131.5 (4C, PhC, DMTr), 129.4 (4C, PhC, DMTr), 128.4(1C, PhC, DMTr), 114.5 (4C, PhC, DMTr), 106.5 (1C, Ar-CH₃, Ar), 88.8 (1C, 1'-C), 88 (1C, CH₂-O-C), 87.2-86.9 (1C, 4'-C), 74 (1C, 3'-C), 64.1 (1C, 5'-C), 60.1-59.5 (1C, P-O-CH₂-CH₂), 56.3 (2C, 2 OCH₃), 46.6-46.2 (2C, 2 P-N-CH-CH₃), 44.7-44.3 (1C, 2'-C), 25.5-23.3 (4C, 4 P-N-CH-CH₃), 21.7-20.9 (1C, P-O-CH₂-CH₂), 17.1(1C, Ar-CH₃), N.B. ^{13}C signature of -CN was not observed as the signal is buried in the -CN peak of the solvent CD_3CN . ^{31}P NMR (162 MHz, CD_3CN) δ (ppm): 149.5. HRMS (ESI+): calculated for $\text{C}_{42}\text{H}_{50}\text{N}_7\text{O}_7\text{PNa}^+$ [M+Na]⁺: 818.3407, found: 818.3421.

Synthesis of F27 substrates. Standard and specialty phosphoramidites, solid-phase oligonucleotide columns, and chemicals needed for the solid-phase DNA synthesis were purchased from Glen Research. All FAM-labeled substrates were synthesized with a 5'-FAM label. The complementary sequence (Comp27) and F27-5mC substrate were synthesized by Integrated DNA Technologies (IDT). The F27-5mZ substrate was synthesized by Keck Oligonucleotide Synthesis Facility at Yale University. F27-4m5mC, F27-4dm5mC, F27-4mC, and F27-4dmC were synthesized in-house via a combination of solid-phase synthesis and post-synthetic modification via a convertible-nucleoside strategy. Convertible nucleoside 4-(1,2,4-triazolyl)-5-methyl-dU CE phosphoramidite (**3**) was used as the precursor to 4m5mC and 4dm5mC bases (Figure S2, top). Convertible nucleoside 4-(1,2,4-triazolyl)-dU CE phosphoramidite was purchased from Glen Research and used as the precursor to 4mC and 4dmC bases (Figure S6). All in-house DNA oligonucleotides were synthesized on an Applied Biosystems Model 394 DNA/RNA synthesizer using CPG columns in 5'-DMT-on mode. For convertible synthesis of different *N*4-modified cytosines or 5-methylcytosines, oligonucleotide-containing CPG beads were first incubated with aqueous solutions of appropriate amines (methylamine or dimethylamine, both 40% (wt/v) in water) for 2 h and then deprotected overnight under standard conditions

SUPPORTING INFORMATION

using fresh concentrated aqueous NH_3 . Deprotected oligonucleotides were then purified using Glen-Pak DNA purification cartridges (Glen Research), lyophilized, and purified using ion-exchange HPLC. Purified oligonucleotides were run on prewarmed (50 °C) 20% TBE-Urea polyacrylamide gels (PAGE) to confirm purity. The gel was imaged for FAM fluorescence using a Typhoon imager (excitation at 488 nm, emission at 520 nm). In all experiments, the F27 substrate DNA refers to duplexed DNA where the F27 substrate strand was duplexed to a complementary strand (Comp27).^[2]

Restriction enzyme-based analysis of F27-5mZ reaction products. Hybridized F27-5mZ or F27-5mC substrates (200 nM), TET reaction buffer (50 mM HEPES, 100 mM NaCl, 1 mM α KG, 1 mM DTT, 2 mM ascorbic acid, pH 6.5), ferrous ammonium sulfate (75 μ M), and TET2-CS (or enzyme storage buffer for no enzyme controls) (1.6 μ M) were combined and incubated at 37 °C for 1 h. Reaction mixtures were purified by Oligo Clean & Concentrator columns (Zymo Research) and the purified reaction products were either sequentially incubated with T4- β GT enzyme (New England Biolabs, NEB) plus UDP-glucose and then MspI (NEB), or MspI alone, following manufacturer's protocol. Samples were mixed with 2x formamide loading buffer, heat-denatured at 75 °C for 5 min and run on a prewarmed (50 °C) 20% TBE Acrylamide Urea-PAGE for 30 min. The gels were imaged for FAM fluorescence using a Typhoon imager (excitation at 488 nm, emission at 520 nm).

ESI-MS analysis of F27-5mZ and F27-5mC reaction products. For the ESI-MS analysis of the reaction products from F27-5mZ, as described above, the purified product DNA was divided into three equal fractions which were used to generate (i) product alone sample, (ii) T4- β GT-reacted sample, and, (iii) sample modified with the aldehyde reactive probe, ARP- ONH_2 (ThermoFisher). To generate these samples, (ii) T4- β GT and (iii) ARP-labeling reactions were both carried out as per the manufacturer's protocol, and samples were then purified by Oligo Clean & Concentrator columns. For these three fractions of products from F27-5mZ, as well as the purified reaction product from F27-5mC, the samples were then analyzed by ESI-MS at Novatia LLC with LC separation (Newtown, PA), with parent DNA masses determined based on the observed masses and abundance of multiply charged species.

ESI-MS analysis of the reaction products of F27-4m5mC, F27-4dm5mC, F27-4mC and F27-4dmC. Hybridized F27-4m5mC, F27-4dm5mC, F27-4mC, and F27-4dmC substrates (400 nM), TET reaction buffer (50 mM HEPES, 100 mM NaCl, 1 mM α KG, 1 mM DTT, 2 mM ascorbic acid, pH 6.5), ferrous ammonium sulfate (75 μ M), and TET2-CS, TET1-FCD, or TET3-FCD (or enzyme storage buffer for no enzyme controls) (1.6 μ M) were combined and incubated at 37 °C for 1 h. Samples were then purified by the Oligo Clean & Concentrator columns and analyzed by ESI-MS at Novatia LLC (Newtown, PA).

LC-MS/MS analysis of the F27-5mC, F27-4m5mC and F27-4dm5mC reaction products. Hybridized F27-5mC, F27-4m5mC and F27-4dm5mC Substrates (200 nM final), TET reaction buffer (50 mM HEPES, 100 mM NaCl, 1 mM α KG, 1 mM DTT, 2 mM ascorbic acid, pH 6.5), ferrous ammonium sulfate (75 μ M), TET2-

SUPPORTING INFORMATION

CS (or enzyme storage buffer for no enzyme controls) (1.6 μM) were combined and incubated at 37 °C for 1 h. Reaction mixtures were cleaned up by the Oligo Clean & Concentrator kit and quantified using Qubit dsDNA reagent (ThermoFisher). 15 ng of the purified reaction products was then degraded to component nucleosides using 1 μL of Nucleoside Digestion Mix (NEB) in 10 μL total volume for 4 h at 37 °C. The mixture was diluted 10-fold into 0.1% formic acid to a final volume of 20 μL . 5 μL was then loaded onto an Agilent 1200 Series HPLC equipped with a 5 μm , 2.1 \times 250 mm Supelcosil LC-18-S analytical column (Sigma) equilibrated to 45 °C in Buffer A (0.1% formic acid). The nucleosides were separated in a gradient of 0–10% Buffer B (0.1% formic acid, 30% (v/v) acetonitrile) over 8 min at a flow rate of 0.5 mL/min. Tandem MS/MS was performed by positive ion mode ESI on an Agilent 6460 triple-quadrupole mass spectrometer, with gas temperature of 225 °C, gas flow of 12 L/min, nebulizer at 35 psi, sheath gas temperature of 300 °C, sheath gas flow of 11 L/min, capillary voltage of 3,500 V, fragmentor voltage of 70 V, and delta EMV of +1,000 V. Collision energies were 5V for all bases except 5mC and 5caC (10V). MRM transitions were 5mC: 242.1 \rightarrow 126.1, 5caC: 272.1 \rightarrow 156.0, 4m5mC: 256.1 \rightarrow 140.1, 4m5hmC: 272.1 \rightarrow 156.1, 4m5fC: 270.1 \rightarrow 154.1, 4m5caC: 286.1 \rightarrow 170.1, 4dm5mC: 270.1 \rightarrow 154.1, and 4dm5caC: 300.1 \rightarrow 184.1.

MspI restriction enzyme assay for F27-5mC, F27-4mC, and F27-4dmC substrates. Hybridized F27-5mC, F27-4mC, or F27-4dmC substrates (100 nM) were incubated with MspI (NEB) following manufacturer protocols. Samples were mixed with 2x formamide loading buffer, heat-denatured at 75 °C for 5 min and run on a prewarmed (50 °C) 20% TBE Acrylamide Urea-PAGE for 30 mins. The gels were imaged for FAM fluorescence using a Typhoon imager (excitation at 488 nm, emission at 520 nm).

Quantitative kinetic analysis of the F27-5mC, F27-5mZ and F27-4dmC substrates with MspI assay. F27-5mC, F27-5mZ, or F27-4dmC substrates (200 nM), TET reaction buffer (50 mM HEPES, 100 mM NaCl, 1 mM DTT, 2 mM ascorbic acid, 1 mM αKG , pH 6.5), ferrous ammonium sulfate (75 μM) and TET2-CS (enzyme serially diluted to 1600 nM, 800 nM, 400 nM, 200 nM, 100 nM, 50 nM, 25 nM, 12.5 nM, 6.25, 0 nM (storage buffer)) were combined and incubated at 37 °C for 1 h. The reactions with F27-5mC and F27-5mZ also contained T4- βGT and UDG-glucose. All reactions were performed in triplicate. DNA samples were purified using the Oligo Clean and Concentrator kit and then digested using MspI (NEB) following the manufacturer's protocol. Samples were mixed with 2x formamide loading buffer, heat-denatured at 75 °C for 5 min, and run on a prewarmed (50 °C) 20% TBE Acrylamide Urea-PAGE for 30 min. The gels were imaged for FAM fluorescence using a Typhoon imager (excitation at 488 nm, emission at 520 nm). Substrate and product bands were quantified using ImageJ, with background correction. Subsequently, data were plotted using Prism software and fitted to sigmoidal log-scale plots to determine various kinetic parameters.

ESI-MS analysis of reaction with B14-6mA RNA. A biotin-labeled 14mer RNA oligonucleotide containing a single N6-methyladenine (B14-6mA) was generously provided by Dr. Kathy Fange Liu with the sequence as noted in Table S1. Single-stranded B14-6mA substrate (400 nM), TET reaction buffer (50 mM HEPES, 100 mM NaCl, 1 mM αKG , 1 mM DTT, 2 mM ascorbic acid, pH 6.5), ferrous ammonium sulfate (75 μM), and TET2-CS (or enzyme storage buffer for no enzyme controls) (1.6 μM) were combined and incubated at 37 °C

SUPPORTING INFORMATION

for 1 h. B14-6mA reaction products were ethanol precipitated. Purified RNA oligonucleotides were then analyzed by ESI-MS at Novatia LLC (Newtown, PA).

SUPPORTING INFORMATION

Supporting Information Figures

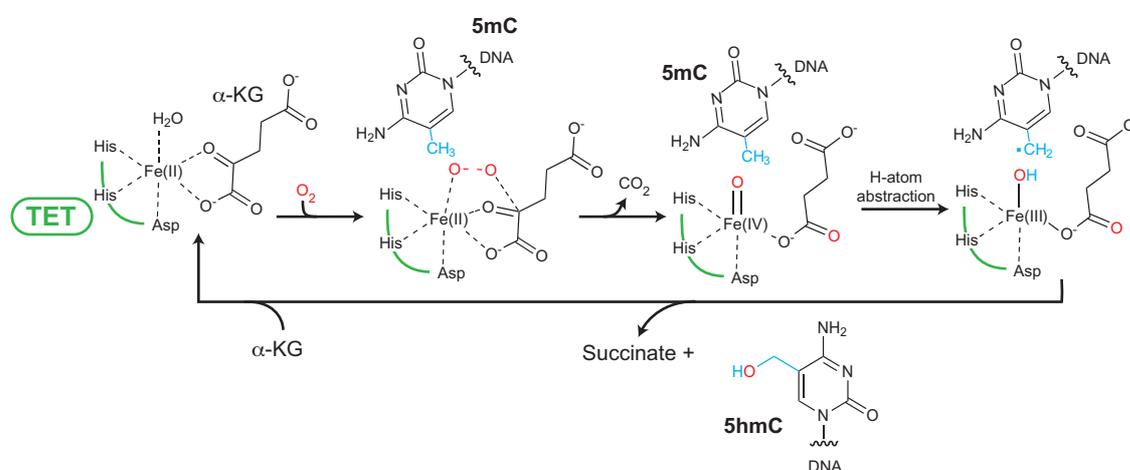


Figure S1. Reaction mechanism for TET-dependent oxidation of 5mC-containing DNA. Shown is the reaction mechanism involving formation of a reactive Fe(IV)-oxo intermediate in proximity to the 5-methyl substituent of 5mC. Notably, with *N*4-methylated analogues used in this study, the methyl substituent on the exocyclic amine may reorient the substrate due to steric clash and provides additional potentially abstractable protons in proximity to the reactive Fe(IV)-oxo intermediate.

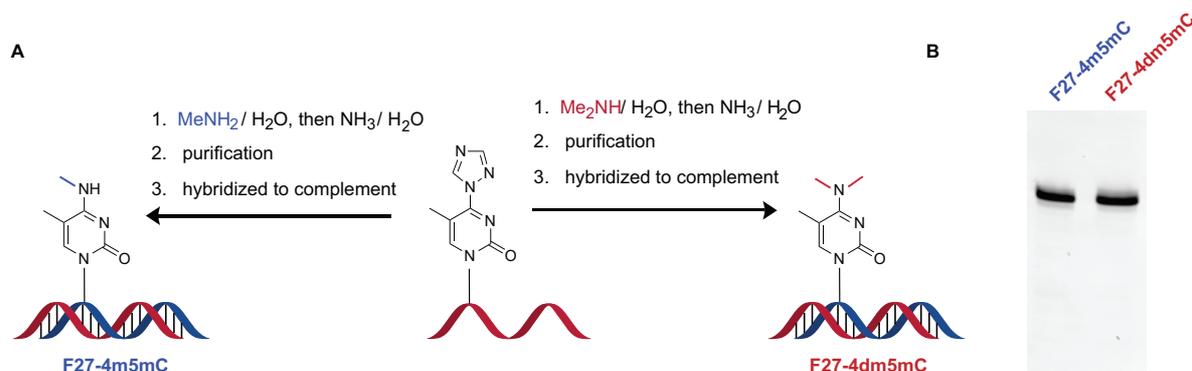


Figure S2. Synthesis of F27-4m5mC and F27-4dm5mC substrates. (A) A convertible nucleoside 4-(1,2,4-triazolyl)-5-methyl-dU (X) was installed in a CXGG sequence context in a 27mer 5'-fluorescein(FAM)-labeled DNA oligonucleotide by solid-phase synthesis. The CPG-bound and protected oligonucleotide was then incubated with the appropriate aqueous amine, and subsequently deprotected with aqueous ammonia to yield crude DNA substrate. Oligonucleotides were purified by HPLC to yield a substrate containing the 4-modified 5-methylcytosine base. (B) Analysis of F27-4m5mC and F27-4dm5mC substrates by denaturing PAGE.

SUPPORTING INFORMATION

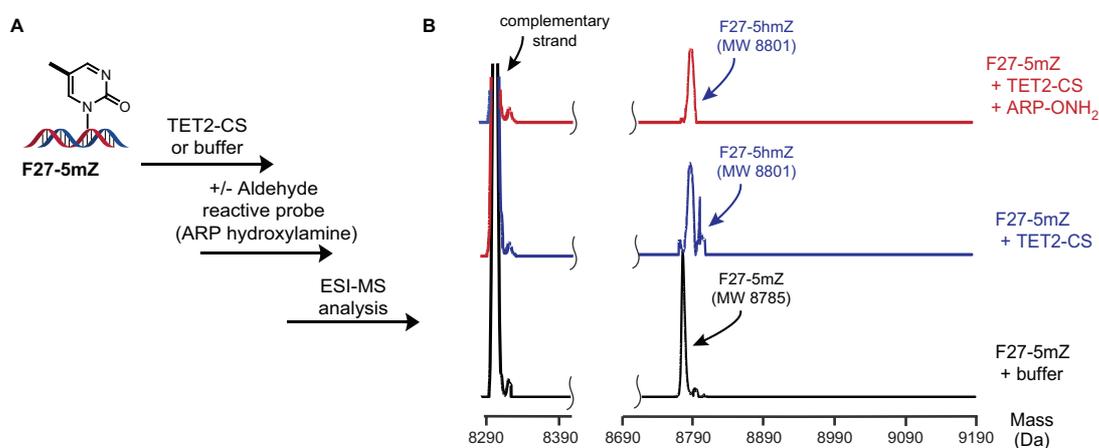


Figure S3. ARP derivatization of F27-5mZ reaction products. (A) Schematic presentation of the analytical procedure. Briefly, F27-5mZ was treated with either storage buffer or TET2-CS and reaction products were purified. TET2-reacted sample was divided into equal fractions and incubated in presence or absence of aldehyde reactive probe, ARP hydroxyl amine (ARP-OH₂). Samples were then purified and subjected to ESI-MS analysis. (B) ESI-MS traces were normalized to the complementary strand and scaled to fit in the figure appropriately. The identities of the labeled masses correspond to those in Table S1. A fragmented x-axis is shown for detected masses given the molecular weight difference between the complementary strand and the substrate strand due to the 5'-FAM label. The absence of a new product upon incubation with ARP-OH₂ supports the conclusion that F27-5mZ oxidation largely stalls at 5-hydroxymethylzebularine (F27-5hmZ).

SUPPORTING INFORMATION

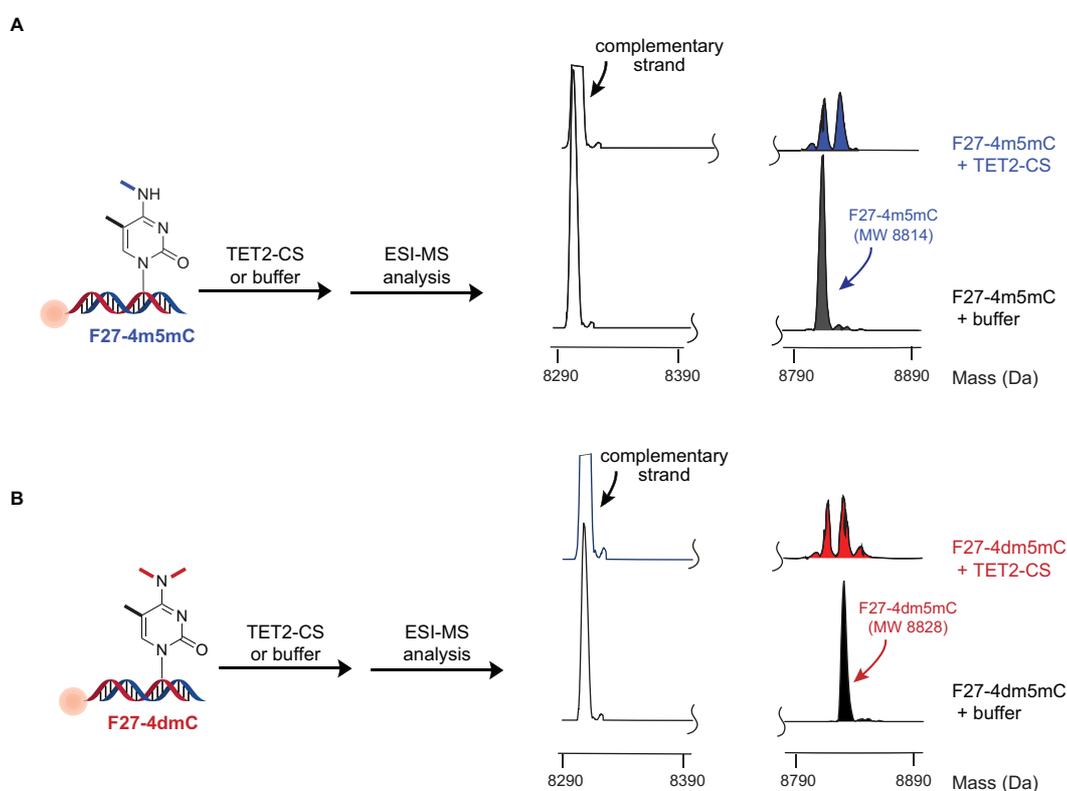


Figure S4. ESI-MS analysis of F27-4m5mC and F27-4dm5mC reaction products. The ESI-MS-based analysis of product formation with either (A) F27-4m5mC or (B) F27-4dm5mC are shown. For each, on the left is the schematic presentation of the analytical procedure. The substrates were treated with either storage buffer or TET2-CS, purified, and subjected to ESI-MS analysis. On the right, the spectral traces are normalized to the complementary strand and scaled to fit in the figure appropriately. The identities of the labeled masses correspond to those in Table S1. New products with both higher and lower masses are detected in the presence of TET2-CS, suggesting the possibility of *N*-demethylation.

SUPPORTING INFORMATION

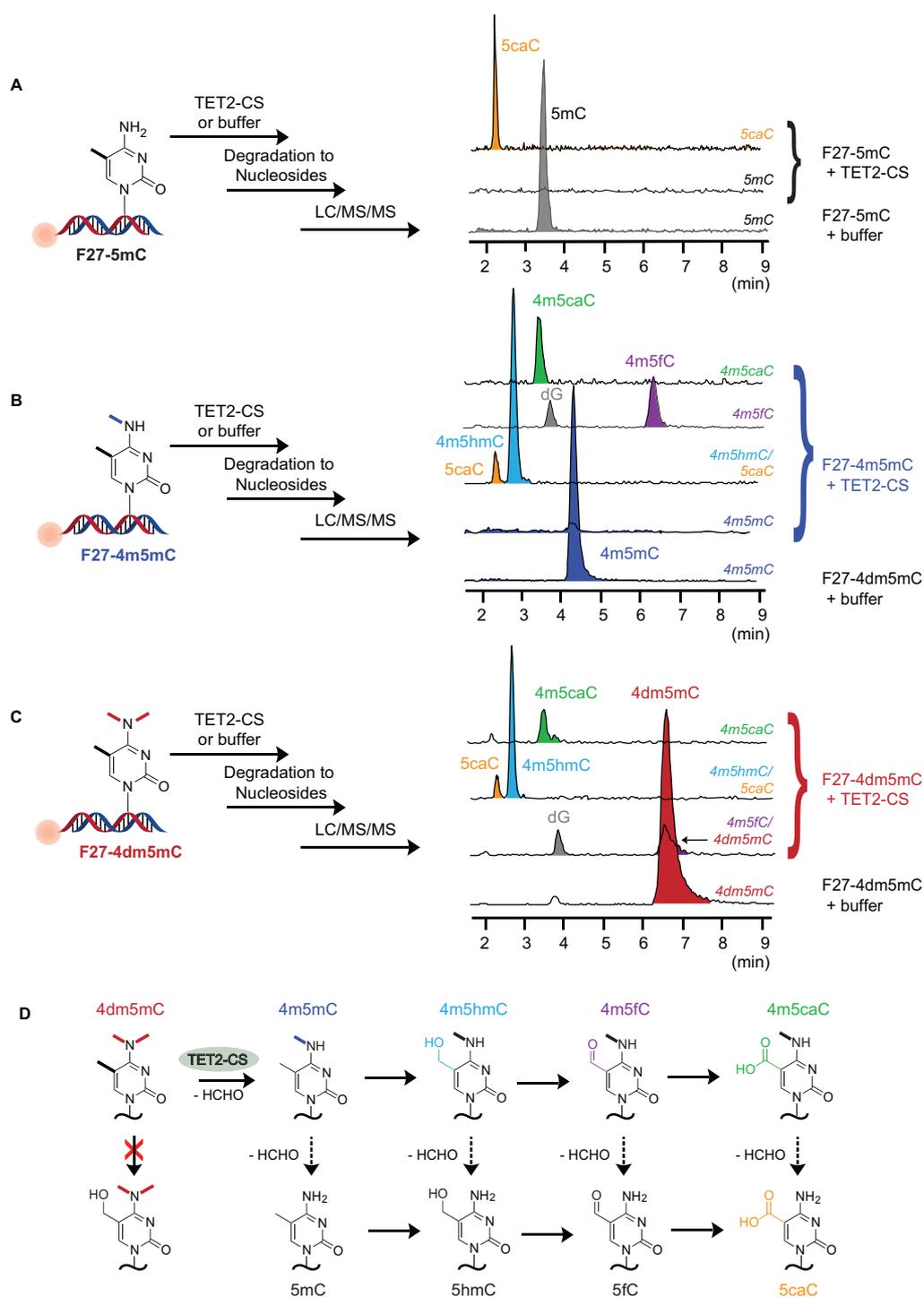


Figure S5. LC-MS/MS analysis of nucleoside products generated from reaction of TET2-CS with F27-5mC, F27-4m5mC and F27-4dm5mC. The LC-MS/MS-based analysis of product formation with either (A) F27-5mC, (B) F27-4m5mC, or (C) F27-4dm5mC are shown. For each substrate, a schematic presentation of the analytical procedure is shown on the left. The substrates were treated with either storage buffer or TET2-CS, purified, degraded to individual nucleosides, and then subjected to LC-MS/MS analysis. The samples were analyzed in multiple reaction monitoring mode (MRM). Selective

SUPPORTING INFORMATION

individual traces are shown, representing fragmentation ions consistent with the mass identities noted on the right in italics. Only traces shown in part (A) had available chemical standards confirming the retention times and mass fragmentation pattern of each nucleoside.² Substrates (4m5mC and 4dm5mC) could also be confirmed by the retention time and mass fragmentation pattern in reactions with buffer only. For the other peaks shown in (B) and (C), the speculative assignment was performed based on mass detection and retention times observed. The bottom trace of each sequence shows the substrate nucleoside starting material and the second from bottom trace in each sequence shows depletion of this nucleoside upon reaction with TET2-CS. For (B), a separate trace consistent with 4m5fC is shown. For (C), given that the mass and retention time of the putative 4m5fC product overlap with the 4dm5mC substrate these are combined in a single trace. Not all detected products are shown and traces lacking an associated mass are not shown for simplicity (e.g. no mass detected consistent with 4dm5hmC). (D) Shown are the possible reaction schematics for conversion of F27-4dm5mC or F27-4m5mC upon reaction with TET2-CS. The detected products noted in colors correspond to the traces in (A-C). For these more complex substrates with multiple reaction possibilities, it is unclear which oxidation and deformylation reaction is most prominent (dashed-lines). ESI-MS and LC-MS/MS analysis on these complex substrates and subsequent experiments with 4mC- and 4dmC-containing simpler substrates collectively establish the occurrence and proficiency of *N*-demethylation.

SUPPORTING INFORMATION

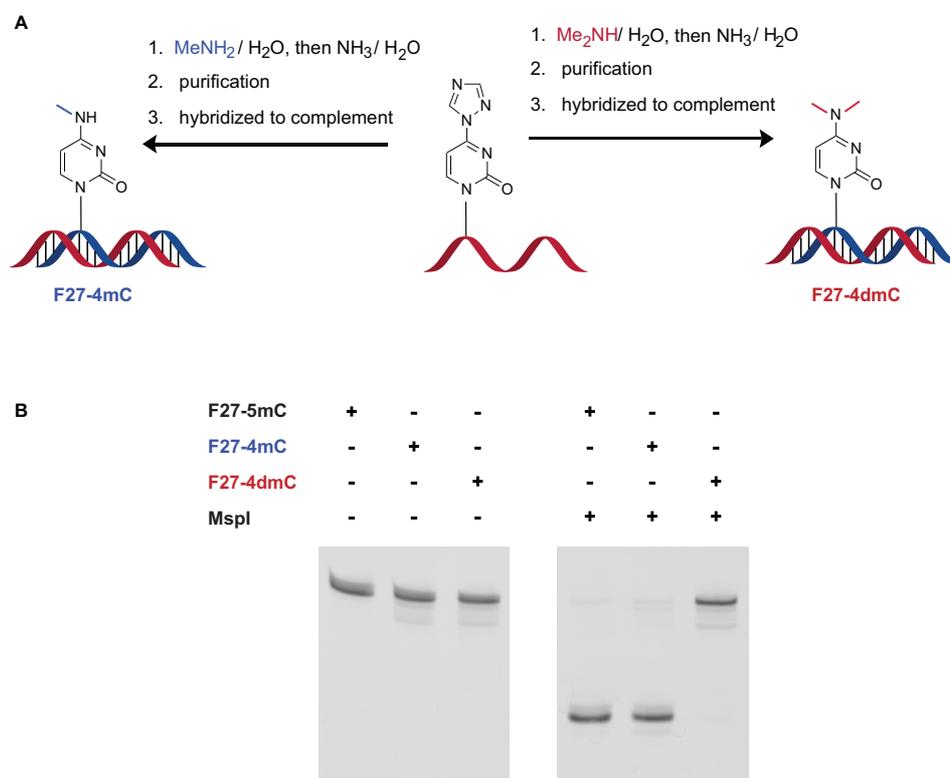


Figure S6. Synthesis and characterization of F27-4mC and F27-4dmC substrates. (A) A convertible 4-(1,2,4-triazolyl)-dU nucleoside (Y) was installed in a CYGG sequence context in a 27mer 5'-fluorescein(FAM)-labeled DNA oligonucleotide. The CPG-bound and protected oligonucleotide was then incubated with the appropriate aqueous amine, and subsequently deprotected with aqueous ammonia to yield crude DNA substrate. Oligonucleotides were purified by HPLC to yield the desired substrate. (B) Analysis of F27-4mC and F27-4dmC substrates. The purified substrates are shown on the left. On the right, the purified duplexes are treated with MspI, showing that the substrate containing 4dmC is protected from cleavage, while a 4mC-containing substrate is cleaved. This selectivity permits the creation of the quantitative demethylation assay used in Figure 3.

SUPPORTING INFORMATION

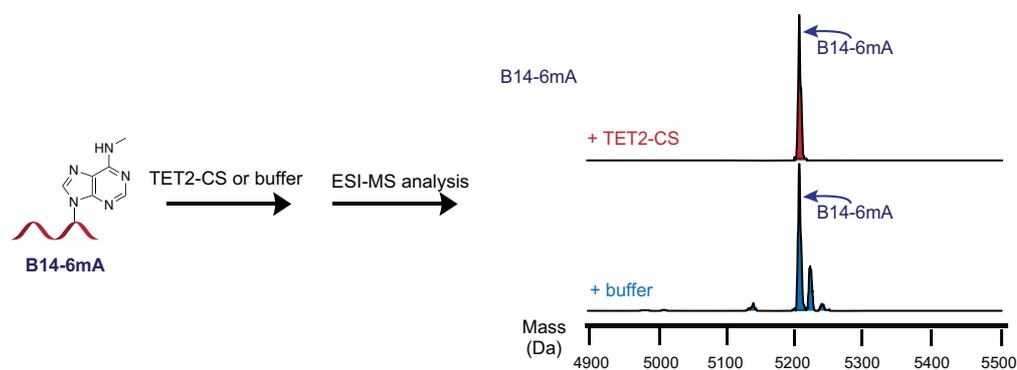
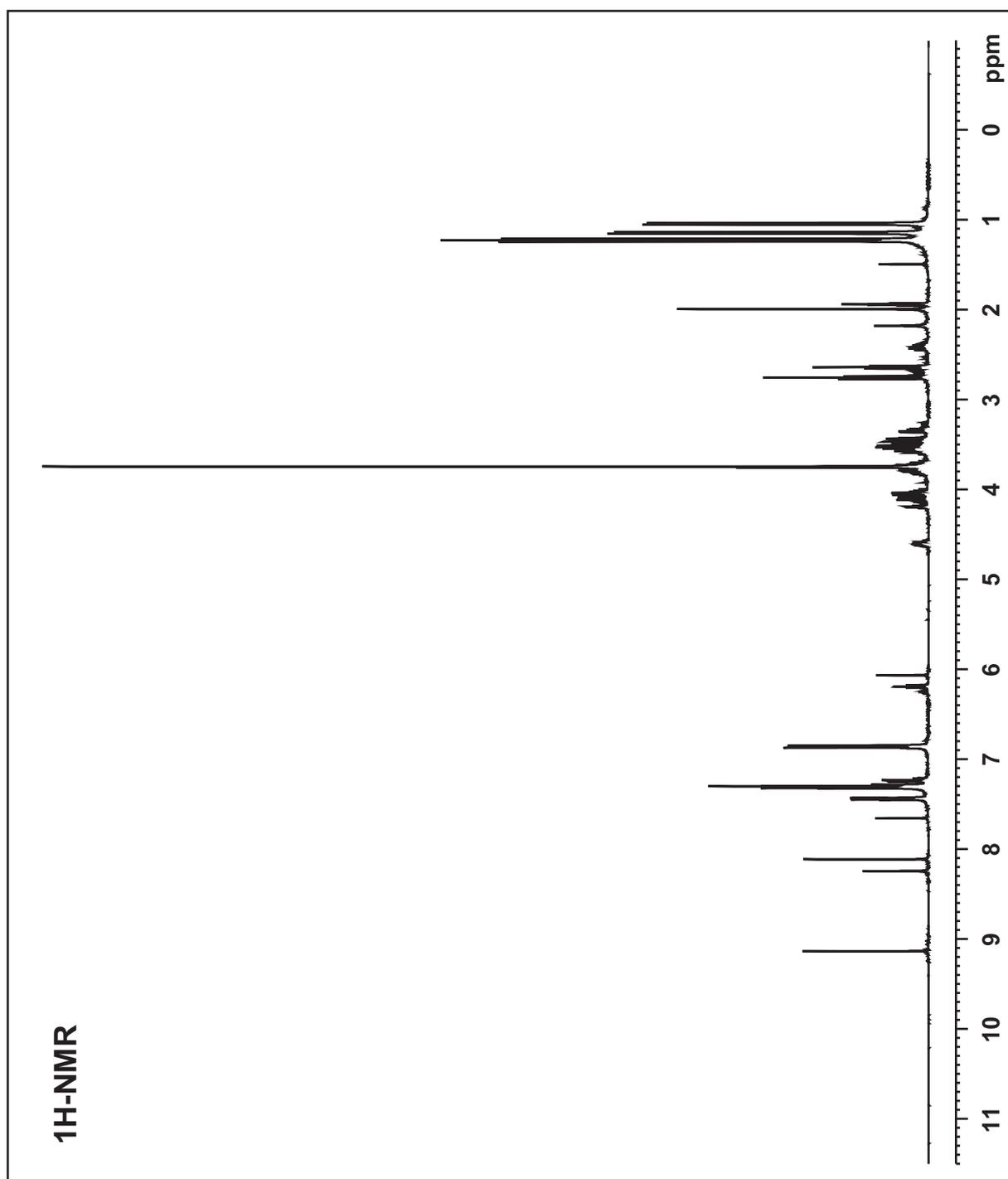


Figure S7. ESI-MS analysis of TET reaction with potential alternative substrate. The ESI-MS-based analysis of product formation with B14-6mA is shown. On the left is the schematic presentation of the analytical procedure. The substrate was treated with either storage buffer or TET2-CS, purified, and subjected to ESI-MS analysis. On the right, the spectral traces are normalized to the maximal peak height and scale to fit in the figure appropriately. The identities of the labeled masses correspond to those in Table S1. No detectable products with lesser masses are observed.

A



B

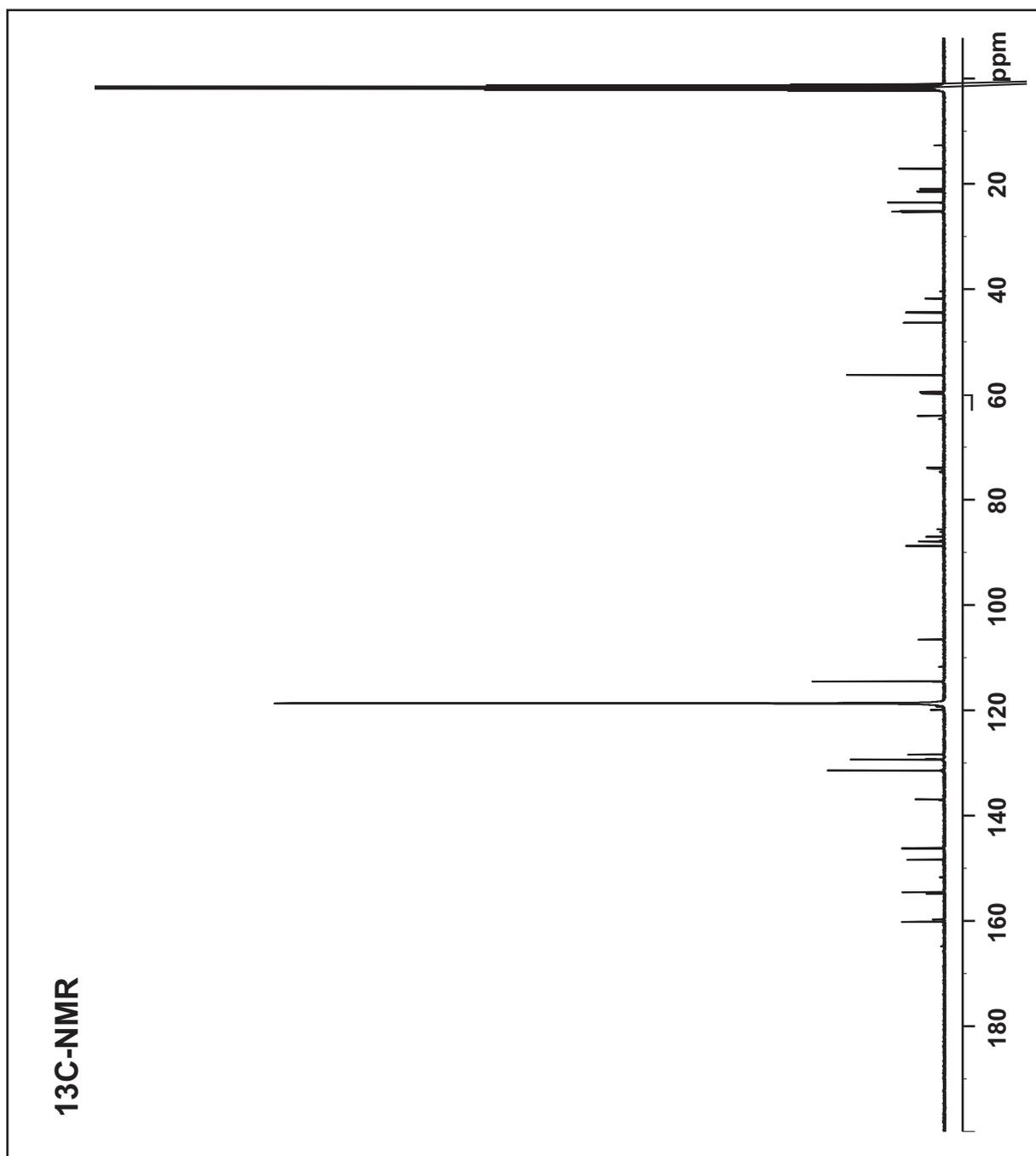


Figure S8. Characterization of convertible 4-(1,2,4-triazolyl)-5-methyl-dU phosphoramidite. (A) ^1H NMR spectra and (B) ^{13}C NMR spectra of the 3'-O-(*N,N*-diisopropylamino-*O*- β -cyanoethoxyphosphino)-5'-O-(4,4'-dimethoxytrityl)-2'-deoxy-5-methyl-4-(1,2,4-triazolyl)-Uridine CE phosphoramidite are shown.

SUPPORTING INFORMATION

Supporting Information Tables

Table S1. ESI-MS characterization of the potential substrates and products.

Name	Sequence	Calc. Mass	Obs. Mass	Synthesized
Substrates				
F27-5mC	5'- FAM-GTA TCT AGT TCA ATC 5mCGG TTC ATA GCA -3'	8801	8802	IDT
F27-5mZ	5'- FAM-GTA TCT AGT TCA ATC 5mZGG TTC ATA GCA -3'	8785	8785	Keck
F27-4m5mC	5'- FAM-GTA TCT AGT TCA ATC 4m5mCGG TTC ATA GCA -3'	8814	8814	In-house
F27-4dm5mC	5'- FAM-GTA TCT AGT TCA ATC 4dm5mCGG TTC ATA GCA -3'	8828	8827	In-house
F27-4mC	5'- FAM-GTA TCT AGT TCA ATC 4mCGG TTC ATA GCA -3'	8829	8829	In-house
F27-4dmC	5'- FAM-GTA TCT AGT TCA ATC 4dmCGG TTC ATA GCA -3'	8843	8844	In-house
Comp27	3'- CAT AGA TCA AGT TAG GCC AAG TAT CGT -5'	8307	8306	IDT
B14-6mA	5'- Biotin-AUG UAG 6mACA GCA GC -3'	5209	5207	Gift from KFL
Products				
F27-5hmZ	5'- FAM-GTA TCT AGT TCA ATC 5hmZGG TTC ATA GCA -3'	8801	8801	
F27-5ghmZ	5'- FAM-GTA TCT AGT TCA ATC 5ghmZGG TTC ATA GCA -3'	8963	8964	
F27-4mC	5'- FAM-GTA TCT AGT TCA ATC 4mCGG TTC ATA GCA -3'	8829	8829	
F27-C	5'- FAM-GTA TCT AGT TCA ATC CGG TTC ATA GCA -3'	8815	8816	

Supporting Information References

- [1] M. Y. Liu, H. Torabifard, D. J. Crawford, J. E. DeNizio, X. J. Cao, B. A. Garcia, G. A. Cisneros, R. M. Kohli, *Nat. Chem. Biol.* **2017**, *13*, 181-187.
- [2] J. E. DeNizio, M. Y. Liu, E. M. Leddin, G. A. Cisneros, R. M. Kohli, *Biochemistry* **2019**, *58*, 411-421.
- [3] M. Saudi, J. Zmurko, S. Kaptein, J. Rozenski, J. Neyts, A. Van Aerschot, *Eur. J. Med. Chem.* **2014**, *76*, 98-109.